Proceedings of the
44th IEEE Conference on Decision and Control, and
the European Control Conference 2005
Seville, Spain, December 12-15, 2005

Power Management Decoupling Control for a Hybrid Electric Vehicle

Osvaldo Barbarisi*, Eric R. Westervelt§, Francesco Vasca* and Giorgio Rizzoni§

*Dipartimento di Ingegneria, Università del Sannio, Piazza Roma 21, 82100 Benevento, Italy;
E-mail: {barbarisi,vasca}@unisannio.it. – http://www.grace.ing.unisannio.it.
§Center for Automotive Research, The Ohio State University, 930 Kinnear Rd, Columbus, Ohio 43212, USA
E-mail: {westervelt.4,rizzoni.1}@osu.edu.

Abstract— **The control of power flow in a Hybrid Electric Vehicle (HEV) is challenging because of the hybrid structure of the driveline and conflicting performance objectives: fuel consumption minimization, state of charge (SOC) regulation, and drivability. The flexibility and dynamic reconfigurability of modern HEV driveline architectures enable the design of power management control strategies that are able to better address these issues. A decoupling control strategy based on such a driveline model is presented. The driveline has three power sources: an internal combustion engine, an integrated starter alternator, and an electric machine. The power management control strategy consists of a control based upon static minimization of the equivalent fuel cost combined with dynamic control of battery SOC and drivability. By exploiting the structure of the driveline's dynamic model, decoupling is obtained in the sense that the battery SOC and drivability controls do not affect the power request constraint, nor do they affect each other.**

I. Introduction

Hybrid Electric Vehicles (HEVs) are gaining in popularity and becoming widespread in large scale industrial production. As a result, there has been increasing research interest in efficient HEV driveline configurations and in the design of corresponding control strategies. In this framework, one of the most important problems is the control of power flow among the different power sources of the vehicle. After vehicle configuration definition and sizing of the components, design of an effective power management control strategy is key for an efficient HEV. The power management control must ensure performance under varying vehicle operating conditions and driver characteristics, such as road grade, vehicle payload, and (possibly aggressive) acceleration and braking commands. The primary object of the control is satisfaction of the driver's power demand. The control must transform driver power demand into the torques that the vehicle's power sources must generate while achieving several other goals, for example, drivability, fuel consumption minimization and regulation of the battery State Of Charge (SOC). The control must also satisfy various constraints on, for example, power source torque demand and speed.

Among the non-heuristic approaches proposed in the literature for the solution of the power management control problem, optimization techniques take the largest part. The existing contributions can be classified as dynamic or static approaches, depending on whether or not dynamic model of the system is explicitly used for formulation and solution of the optimization problem. Dynamic approaches are typically based on dynamic programming or optimization on a receding time horizon [1], [2], [3]. In order to be implemented, dynamic solutions require knowledge of the future driving profile, which is impossible. To circumvent this problem, representative driving cycles are used in design; however, such cycles are not sufficiently rich to capture all vehicle conditions. Static approaches are based mainly on the Equivalent fuel Consumption Minimization Strategy (ECMS) [4], which can be adapted to also consider battery SOC and emissions constraints [5], [6]. One of the drawbacks of the static approach is that some important dynamic effects, such as those related to drivability and battery SOC variations [7], cannot be explicitly treated. A comparison between dynamic and static approaches for the power management control has been analyzed recently [8], [9].

The control strategy proposed in this paper deals with power management control from a different perspective. By exploiting the dynamic model of the HEV driveline, it is shown that the control signal can be separated into three components. The first component is dedicated to the satisfaction of the driver power request and is designed by using an ECMS procedure. The second component is devoted to the control of battery SOC. The third component is used to ensure drivability. The control components are decoupled in the sense that the last two components do not affect the power request, the second component does not affect drivability, and the third component does not affect the battery SOC.

Sec. II gives the HEV driveline model treated in this work. The model corresponds to a prototype HEV under construction at The Ohio State University for the Challenge X competition [10]. Sec. III gives the details of the control and a physical interpretation of the decoupling using power flow paths in the HEV. Sec. IV gives a simulation illustrating the effectiveness of the proposed control strategy.

II. Vehicle Concept

The hybrid vehicle under consideration has the parallel architecture depicted in Fig. 1. An Integrated Starter Alternator (ISA) is rigidly attached to the Internal Combustion Engine (ICE). A torque converter is between the ICE-ISA and an automatic transmission that drives the vehicle's front

0-7803-9568-9/05/$20.00 ©2005 IEEE

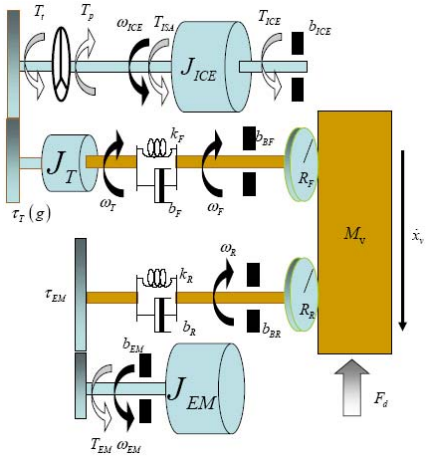

Fig. 1. Architecture of the hybrid electric vehicle driveline considered. The driveline corresponds to that of The Ohio State University's Challenge X prototype.

wheels. Directly driving the rear wheels is an Electric Motor (EM) with gear reducer.

The following assumptions are made regarding the driveline model and underlie the control approach. First, the ICE, ISA, and EM are considered to be actuators in that their torque may be directly commanded. Their interaction with the driveline's model, however, are considered (see (1) below). Second, when considering fuel consumption minimization, the dynamics of the ICE may be ignored. Third, it is assumed that driver is not simultaneously commanding (positive) acceleration and braking at the same instant.

A. Driveline model

By considering the driveline scheme given in Fig. 1 and the above assumptions, the following lumped parameter dynamic model of the driveline may be obtained using the method of Lagrange.

$$\begin{aligned} J_{\mathrm{ICE}}\dot{\omega}_{\mathrm{ICE}} &= -b_{\mathrm{ICE}}\omega_{\mathrm{ICE}} \\ &\quad - T_{\mathrm{p}}(\omega_{\mathrm{ICE}},\omega_{\mathrm{T}}) + T_{\mathrm{ICE}} + T_{\mathrm{ISA}}, && \text{(1a)} \\ J_{\mathrm{T}}\dot{\omega}_{\mathrm{T}} &= \frac{1}{\tau_{\mathrm{T}}(g)}T_{\mathrm{t}}(\omega_{\mathrm{ICE}},\omega_{\mathrm{T}}) - T_{\mathrm{F}}, && \text{(1b)} \\ J_{\mathrm{EM}}\dot{\omega}_{\mathrm{EM}} &= -b_{\mathrm{EM}}\omega_{\mathrm{EM}} - \tau_{\mathrm{EM}}T_{\mathrm{R}} + T_{\mathrm{EM}}, && \text{(1c)} \\ M_{\mathrm{v}}\ddot{x}_{\mathrm{v}} &= \frac{1}{R_{\mathrm{F}}\tau_{\mathrm{DF}}}T_{\mathrm{F}} + \frac{1}{R_{\mathrm{R}}\tau_{\mathrm{DR}}}T_{\mathrm{R}} - \beta\frac{1}{R_{\mathrm{F}}}b_{\mathrm{BF}}\omega_{\mathrm{F}} \\ &\quad - \beta\frac{1}{R_{\mathrm{R}}}b_{\mathrm{BR}}\omega_{\mathrm{R}} - F_{\mathrm{L}}, && \text{(1d)} \\ \dot{s} &= -\frac{1}{s^{\max}}\left(\omega_{\mathrm{ICE}}T_{\mathrm{ISA}} + \omega_{\mathrm{EM}}T_{\mathrm{EM}}\right), && \text{(1e)} \end{aligned}$$

where J_* are inertias, $\omega_* = \dot{\theta}_*$, b_* are coefficients of friction, T_* are torques, τ_* are gear ratios, $g \in \{0,1,\ldots,5\}$ is the automatic transmission's gear index, x_{v} is the vehicle's linear displacement, R_* are wheel radii, $\beta \in [0,1]$ is the normalized mechanical brake command, F_{L} includes vehicle drag and other possible loads, s is the battery SOC where $s \in [0,1]$, p denotes the torque converter pump, T denotes the transmission, t denotes the torque converter turbine, F denotes the front wheels, R denotes the rear wheels, DF denotes the front differential, DR denotes the rear differential, BF denotes the front brakes, and BR denotes the rear brakes. See Table I, given the Appendix, for the parameters' values. The torque converter turbine output torque, T_{t}, and input torque, T_{p}, are assumed to be a quadratic function of the engine and transmission speeds [11]. The load at the front, T_{F}, and rear, T_{R}, wheels is given by

$$\begin{aligned} T_{\mathrm{F}} &= b_{\mathrm{F}}(\omega_{\mathrm{T}} - \omega_{\mathrm{F}}) + k_{\mathrm{F}}(\theta_{\mathrm{T}} - \theta_{\mathrm{F}}), && \text{(2a)} \\ T_{\mathrm{R}} &= b_{\mathrm{R}}(\omega_{\mathrm{EM}}\tau_{\mathrm{EM}} - \omega_{\mathrm{R}}) + k_{\mathrm{R}}(\theta_{\mathrm{EM}}\tau_{\mathrm{EM}} - \theta_{\mathrm{R}}), && \text{(2b)} \end{aligned}$$

where $\omega_{\mathrm{F}} = \frac{\dot{x}_{\mathrm{v}}}{R_{\mathrm{F}}}$ and $\omega_{\mathrm{R}} = \frac{\dot{x}_{\mathrm{v}}}{R_{\mathrm{R}}}$.

B. Constraints

For simplicity, it is assumed that the positive and negative power constraints of the battery are equal and, hence,

$$|\omega_{\mathrm{ICE}}T_{\mathrm{ISA}} + \omega_{\mathrm{EM}}T_{\mathrm{EM}}| \le P_{\mathrm{batt}}, \qquad (3)$$

which also represents a constraint on the derivative of s. To ensure proper functionality of the electronic devices and long battery life, the battery SOC is constrained to a subset of allowable values,

$$s_l \le s \le s_u. \qquad (4)$$

Additional constraints arise from speed limitations of the engine and electric motors,[1]

$$0 \le \omega_{\mathrm{ICE}} \le \omega_{\mathrm{ICE}}^{\max} \quad \text{and} \quad 0 \le \omega_{\mathrm{EM}} \le \omega_{\mathrm{EM}}^{\max}, \qquad (5)$$

and limitations on torque,

$$\begin{aligned} 0 \le T_{\mathrm{ICE}} &\le T_{\mathrm{ICE}}^{\max}(\omega_{\mathrm{ICE}}), && \text{(6a)} \\ T_{\mathrm{ISA}}^{\min}(\omega_{\mathrm{ICE}}) \le T_{\mathrm{ISA}} &\le T_{\mathrm{ISA}}^{\max}(\omega_{\mathrm{ICE}}), && \text{(6b)} \\ T_{\mathrm{EM}}^{\min}(\omega_{\mathrm{EM}}) \le T_{\mathrm{EM}} &\le T_{\mathrm{EM}}^{\max}(\omega_{\mathrm{EM}}). && \text{(6c)} \end{aligned}$$

Although the engine torque, T_{ICE}, may be negative (i.e., the engine may act as a brake), this case is not considered in the constraint because negative engine torque cannot be directly controlled as it only depends on the engine speed. As a result, all braking considered is either regenerative or frictional.

C. Power demand

The driver makes power requests to the driveline by depressing the accelerator pedal or brake pedal, and, by assumption, not both simultaneously. The instantaneous power that may be supplied is

$$\begin{aligned} P_{\mathrm{inst}} &= \omega_{\mathrm{ICE}}T_{\mathrm{ICE}} + \omega_{\mathrm{ICE}}T_{\mathrm{ISA}} + \omega_{\mathrm{EM}}T_{\mathrm{EM}} \\ &\quad - \beta b_{\mathrm{BF}}\omega_{\mathrm{F}}^2 - \beta b_{\mathrm{BR}}\omega_{\mathrm{R}}^2 \end{aligned} \qquad (7)$$

where the maximum and minimum powers that may be requested are

$$\begin{aligned} P^{\max} &= \omega_{\mathrm{ICE}}T_{\mathrm{ICE}}^{\max}(\omega_{\mathrm{ICE}}) + \omega_{\mathrm{ICE}}T_{\mathrm{ISA}}^{\max}(\omega_{\mathrm{ICE}}) \\ &\quad + \omega_{\mathrm{EM}}T_{\mathrm{EM}}^{\max}(\omega_{\mathrm{EM}}), && \text{(8a)} \\ P^{\min} &= \omega_{\mathrm{ICE}}T_{\mathrm{ISA}}^{\min}(\omega_{\mathrm{ICE}}) + \omega_{\mathrm{EM}}T_{\mathrm{EM}}^{\min}(\omega_{\mathrm{EM}}) \\ &\quad - b_{\mathrm{BF}}\omega_{\mathrm{F}}^2 - b_{\mathrm{BR}}\omega_{\mathrm{R}}^2. && \text{(8b)} \end{aligned}$$

[1]For simplicity, only forward driving is considered. Therefore, the EM is assumed to rotate only in the positive direction.

The control receives from the driver only the two pedal commands, $\alpha_D \in [0,1]$, the normalized accelerator pedal angle, and $\beta_D \in [0,1]$, the normalized brake pedal angle, with $\alpha_D \perp \beta_D$ (i.e., α_D and β_D not both simultaneously nonzero). The power requested is defined as the portion of maximum power available as determined by the driver commands,

$$P_{\text{inst}} = \alpha_D P^{\max} + \beta_D P^{\min}. \tag{9}$$

The mechanical brake will be used only in the case the P_{inst} is less then the minimum power available with only the electric machine, in other words, when the regenerative braking is not enough to brake the vehicle.

III. Control Strategy

A. Model reformulation

Define the control $u := \begin{pmatrix} T_{\text{ICE}} & T_{\text{ISA}} & T_{\text{EM}} \end{pmatrix}'$, the state vector $x := \begin{pmatrix} \omega_{\text{ICE}} & \omega_{\text{T}} & \omega_{\text{EM}} & \dot{x}_{\text{v}} & \theta_{\text{T}} & \theta_{\text{EM}} & x_{\text{v}} \end{pmatrix}'$ and $\Gamma := \begin{pmatrix} 0_{1\times 6} & -F_{\text{L}} \end{pmatrix}'$. The system (1) and the constraints can then be rewritten as

$$M\dot{x} = f(x) + Bu + \Gamma \tag{10a}$$
$$\dot{s} = x'Nu \tag{10b}$$
$$x'Bu = P_{\text{inst}} \tag{10c}$$
$$x^{\min} \le x \le x^{\max} \tag{10d}$$
$$u^{\min} \le u \le u^{\max} \tag{10e}$$
$$s_l \le s \le s_u \tag{10f}$$
$$-P_{\text{batt}} \le \dot{s} \le P_{\text{batt}}, \tag{10g}$$

where the box constraints are element-wise, and

$$M = \text{diag}\{J_{\text{ICE}}, J_{\text{T}}, J_{\text{EM}}, M_{\text{v}}, 1, 1, 1\}, \tag{11}$$

$$B = \begin{bmatrix} 1 & 1 & 0 \\ 0 & 0 & 0 \\ 0 & 0 & 1 \\ \hline & 0_{4\times 3} & \end{bmatrix}, \quad N = -\frac{1}{s^{\max}} \begin{bmatrix} 0 & 1 & 0 \\ 0 & 0 & 0 \\ 0 & 0 & 1 \\ \hline & 0_{4\times 3} & \end{bmatrix}. \tag{12}$$

Analysis of the battery SOC dynamics (10b) and of the power constraint (10c) reveals that the control of fuel economy, battery SOC control, and drivability may be decoupled. Null control directions of the battery SOC dynamics (10b),

$$\mathcal{N}(x'N) = \text{span}\left\{ \begin{bmatrix} 1 \\ 0 \\ 0 \end{bmatrix}, \begin{bmatrix} 0 \\ x_3 \\ -x_1 \end{bmatrix} \right\}, \tag{13}$$

and of the power constraint (10c),

$$\mathcal{N}(x'B) = \text{span}\left\{ \begin{bmatrix} 1 \\ -1 \\ 0 \end{bmatrix}, \begin{bmatrix} 0 \\ x_3 \\ -x_1 \end{bmatrix} \right\}, \tag{14}$$

enable the definition of decoupled controls inputs,

$$u_\mu = \begin{bmatrix} 1 \\ -1 \\ 0 \end{bmatrix} \quad \text{and} \quad u_\nu(x) = \begin{bmatrix} 0 \\ x_3 \\ -x_1 \end{bmatrix}. \tag{15}$$

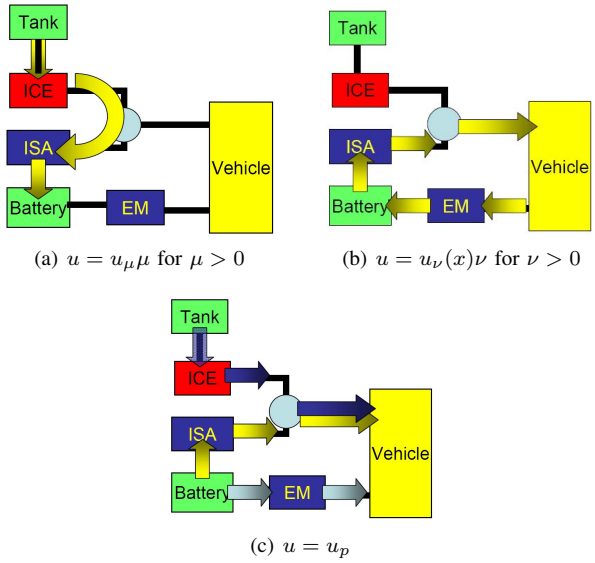

(a) $u = u_\mu \mu$ for $\mu > 0$ (b) $u = u_\nu(x)\nu$ for $\nu > 0$

(c) $u = u_p$

Fig. 2. Energy flow under the three components of control action u.

Hence, if u_p is a solution of (10c), then

$$u = u_p + u_\mu \mu + u_\nu(x)\nu, \tag{16}$$

with $\mu, \nu \in \mathbb{R}$ is as well. Note that $u_\nu(x) \in \mathcal{N}(x'N)$. The model (10) may now be written as

$$M\dot{x} = f(x) + Bu_p + Bu_\nu(x)\nu + \Gamma \tag{17a}$$
$$\dot{s} = x'Nu_p + x'Nu_\mu\mu \tag{17b}$$
$$x'Bu_p = P_{\text{inst}} \tag{17c}$$
$$x^{\min} \le x \le x^{\max} \tag{17d}$$
$$u^{\min} \le u_p + u_\mu\mu + u_\nu(x)\nu \le u^{\max} \tag{17e}$$
$$s_l \le s \le s_u \tag{17f}$$
$$-P_{\text{batt}} \le \dot{s} \le P_{\text{batt}}, \tag{17g}$$

which has three control inputs, $u_p \in \mathbb{R}^3$ and $\mu, \nu \in \mathbb{R}$. The feedforward control u_p is chosen to satisfy the power demand from the driver while considering the efficiency of the ICE, EM and ISA. The controls μ and ν are used to regulate the battery SOC and to maintain drivability, respectively. Vectors u_μ and u_ν represent control directions that exploit the series and parallel hybridization of the vehicle and do not affect the instantaneous power of the vehicle. For $\mu > 0$ fuel is consumed by the ICE, and the ISA is used as a generator to charge the battery;[2] see Fig. 2(a).

Regulation by ν enables power to be transferred between the front and rear wheels such that the battery SOC and the kinetic energy of the vehicle are not affected; see Fig. 2(b). In reality, power will be lost due to the inefficiency of the mechanical and electrical components of the driveline. For this reason, the controls μ and ν will be used only to ensure battery SOC regulation and drivability.

Finally, the feedforward control u_p is used to satisfy the driver's power demand. This portion of the control manages

[2]Since $u_{p,1} > 0$ in general, μ may be negative. Saturation is used to ensure that $T_{\text{ICE}} \ge 0$.

the power split between the ICE, ISA, and EM (see Fig. 2(c)) using the Equivalent fuel Consumption Minimization Strategy (ECMS), which is described next.

B. Fuel consumption minimization

The ECMS procedure [4] is used to minimize the fuel consumed by the HEV by minimizing the fuel or equivalent amount of fuel consumed by each component. It is based upon the fact that all energy consumed by the vehicle, whether mechanical or electrical, comes ultimately from the fuel tank. ECMS is formulated here to compute the feedforward control u_p by

$$u_p = \arg\min_{\bar{u}\in\mathbb{R}^3} \{\dot{m}_{\rm ICE}(x_1,\bar{u}_1) + \dot{m}_{\rm ISA}(x_1,\bar{u}_2) + \dot{m}_{\rm EM}(x_3,\bar{u}_3)\}, \quad (18)$$

subject to the power demand constraint,

$$P_{\rm inst} = x_1\bar{u}_1 + x_1\bar{u}_2 + x_3\bar{u}_3, \quad (19)$$

and the constraints given by (17d), (17e), and (17g) where

$$\dot{m}_*(x_i,\bar{u}_j) = \frac{x_i\bar{u}_j}{\eta_*(x_i,\bar{u}_j)Q_{\rm LHV}}, \quad (20)$$

η_* are the efficiencies, and $Q_{\rm LHV}$ is the low heating value of the fuel.

The control u_p is obtained by performing the optimization on a discretized grid of the set of possible operating states. Since the efficiency maps are obtained at steady state, during transients (18) will represent a sub-optimal solution. However, it is important to note that the constraint (19) is satisfied at every time instant, which is important because $P_{\rm inst}$ represents the driver demand and is the primary request to be satisfied.

C. Battery SOC control

By using the control component u_μ it is possible to control the battery SOC without affecting the constraint on the power demand, (17c) and (17b). Application of the control

$$\mu = \frac{s^{\max}}{x_1}K_v(s_m - s), \quad (21)$$

where $s_m = (s_l + s_u)/2$ and definition of $\tilde{s} := s - s_m$, results in battery SOC dynamic

$$\dot{\tilde{s}} = -\frac{1}{s^{\max}}(P_{\rm inst} - x_1u_{p,1}) - K_v\tilde{s}. \quad (22)$$

Note that (21) is well-defined since the ICE speed, x_1, is nonzero whenever the ICE is running. While the origin of the battery SOC dynamic (22) is not asymptotically stable, due to the non-vanishing perturbation $-(P_{\rm inst} - x_1u_{p,1})/s^{\max}$, regulation of $\tilde{s}$ to a small set is possible with appropriate choice of K_v. Note that the control

$$\bar{\mu} = \frac{1}{x_1}(P_{\rm inst} - x_1u_{p,1}) - \frac{s^{\max}}{x_1}K_v\tilde{s}, \quad (23)$$

would result in the battery SOC dynamic, $\dot{\tilde{s}} = -K_v\tilde{s}$, which does have the origin as an asymptotically stable equilibrium point. However, it is impractical since its application annihilates the ECMS-based control and thus all associated performance characteristics would be lost.

D. Driveability control

Smooth gear shifting is assumed to be the main goal for achieving good drivability.[3] In particular, the control objective is to minimize the difference between engine speed, $x_1 = \omega_{\rm ICE}$, and turbine speed of the torque converter, $x_2/\tau_{\rm T}(g) = \omega_{\rm T}/\tau_{\rm T}(g)$. This will be achieved using a gain-scheduled, infinite horizon LQR regulator.

The regulator design proceeds by first linearizing the vehicle dynamics, (17a),

$$\delta\dot{x} = A_\nu\delta x + B_\nu\delta\nu \quad (24)$$

where

$$A_\nu(g,x_1,x_2) = M^{-1}\frac{\partial f(x)}{\partial x} + M^{-1}B\frac{\partial u_\nu}{\partial x}, \quad (25a)$$

$$B_\nu(x_1,x_3) = M^{-1}Bu_\nu. \quad (25b)$$

The cost function to be minimized is

$$J(g,x_1,x_2,\nu) = \int_0^\infty \left[\left(x_1 - \frac{x_2}{\tau_{\rm T}(g)}\right)^2 + \rho\,\nu^2\right]dt, \quad (26)$$

where $\rho > 0$. The infinite horizon LQR regulator that minimizes J is calculated on a discretized grid of g, x_1, x_2, and x_3. At each grid point, controllability of the linearized model with respect to ν is verified, and the Riccati equation,

$$A_\nu'P + PA_\nu - \frac{1}{\rho}PB_\nu B_\nu'P + Q = 0 \quad (27)$$

with

$$Q = \left[\begin{array}{cc|c} 1 & -\frac{1}{\tau_{\rm T}(g)} & \\ -\frac{1}{\tau_{\rm T}(g)} & \frac{1}{\tau_{\rm T}^2(g)} & 0_{2\times5} \\ \hline & 0_{5\times2} & 0_{5\times5} \end{array}\right], \quad (28)$$

is solved for P. The resulting controller is

$$\delta\nu = -K'(g,x_1,x_2,x_3)\delta x \quad (29)$$

with

$$K' = -\frac{1}{\rho}B_\nu'P(g,x_1,x_2,x_3). \quad (30)$$

Note that the gain K depends only on the gear selected and x_1, x_2 and x_3. For implementation, $K(g,x_1,x_2,x_3)$ is computed off-line to generate a lookup table.

IV. Simulation result

The control strategy described in Sec. III was simulated for the model given in Sec. II for a typical highway driving cycle lasting 400 seconds. Fig. 3 gives desired and actual vehicle speeds for the driving cycle. The command of the driver, which is modeled as a PI controller on the difference between the desired and actual vehicle speeds, is given in Fig. 4. Figs. 5, 6 and 7 give the ICE, ISA, and EM torque. Figs. 8 and 9 give the ICE (which is also the ISA speed) and EM speeds. Fig. 10 gives the transmission gear selected.[4] Fig. 11

[3] Another source of poor drivability is ICE lag in torque production which it is not considered for the sake of simplicity.

[4] The gear of the automatic transmission is indexed (resp. decremented) when the engine speed exceeds (resp. falls below) pre-determined values for a given time duration.

gives the battery SOC. Fig. 12 gives the instantaneous power demand, and the maximum and minimum instantaneous power possible.

V. Conclusions

A power management control strategy of an HEV was presented. Exploiting decoupling that is inherent to the driveline, the control strategy is broken into three parts: 1) a static power management control strategy based upon ECMS; 2) a dynamic control of battery SOC; and 3) a dynamic control to ensure drivability. These controls are decoupled in the sense that the battery SOC and drivability controls do not affect the power request constraint, and the battery SOC and drivability controls do not affect drivability and battery SOC, respectively. The control strategy ensures that the power demand of the driver is met, resulting in the sensation of one power source though three are utilized.

Future work includes improved battery SOC regulation, inclusion of engine combustion dynamics, the control necessary to ameliorate the associated drivability issues, and implementation on the prototype vehicle.

References

[1] C.-C. Lin, H. Peng, J. W. Grizzle, and J.-M. Kang, "Power management strategy for parallel hybrid electric truck," *IEEE Trans. on Control systems Technology*, vol. 11, no. 6, pp. 839–849, 2003.

[2] G. Steinmauer and L. del Re, "Optimal control of dual power sources," in *Proc. of IEEE Conference on Control Applicarions*, Mexico City, Mexico, 2001.

[3] A. Brahma, Y. Guezennec, and G. Rizzoni, "Dynamic optimization of mechanical/electrical power flow in parallel hybrid electric vehicles," in *Proc. of 5th Int. Symposium Advanced Vehicle Control*, Anna Arbor, Michigan, 2000.

[4] G. Paganelli, G. Ercole, A. Brahma, Y. Guezennec, and G. Rizzoni, "General supervisory control policy for the energy optimization of charge-sustaining hybrid electric vehicles," *Journal of Society of Automotive Engineers of Japan*, vol. 22, 2001.

[5] A. Sciarretta, M. Back, and L. Guzzella, "Optimal control of parallel hybrid electric vehicles," *IEEE Trans. on Control Systems Technology*, vol. 12, no. 3, pp. 352–363, 2004.

[6] V. H. Johnson, K. B. Wipke, and D. J. Rausen, "Hev control strategy for real-time optimization of fuel economy and emissions," in *Proc. of Future Car Congress 2000-01-1543*, Arlington, Virginia, 2000.

[7] X. Wei, P. Pisu, G. Rizzoni, and S. Yurkovich, "Dynamic modelinf of a hybrid electric drivetrain for fuel economy, performance and driveability evaluations," in *Proc. of ASME Int. Mechanical Engineering Congress*, Washington D.C., USA, 2003.

[8] Y. Zhu, Y. Chen, G. Tian, H. Wu, and Q. Chen, "A four-step method to design an energy managemnt strategy for hybrid vehicles," in *Proc. of American Control Conference*, Boston, Massachusetts, 2004.

[9] P. Pisu, C. Musardo, G. Rizzoni, and B. Scaccia, "A comparative study of supervisory control strategies for hybrid electric vehicles," in *Proc. of ASME Int. Mechanical Engineering Congress*, Anaheim, California, 2004.

[10] "Challenge X website," 2005, http://www.challengex.org/.

[11] H. L. Kin-Hyuk Lee, "Dynamic simulation of nonlinear model-based observer for hydrodynamic torqueconverter system," in *SAE 2004 World Congress and Exhibition*, Detroit, Michigan, USA.

[12] M. Best, "Nonlinear optimal control of vehicle driveline vibrations," in *IEE International Conference on Control*, 1998, pp. 658–63.

Appendix

A. Model parameters

The model parameters are given in Table I are taken from [12] and from the component manufactures' data sheets for a prototype HEV under construction at The Ohio State University for the Challenge X competition [10]. Note, by convention $1/\tau_{\rm T}(0) := 0$.

Parameter	Symbol	Value
Vehicle mass	$M_{\rm v}$	1310 kg
ICE inertia	$J_{\rm ICE}$	3.544 kg-m^2
Transmission inertia	$J_{\rm T}$	1.340 kg-m^2
EM inertia	$J_{\rm EM}$	5.340 kg-m^2
ICE viscous damping	$b_{\rm ICE}$	0.012 N-m-s/rad
EM viscous damping	$b_{\rm EM}$	0.20 N-m-s/rad
Frictional brake constants	$b_{\rm BF} = b_{\rm BR}$	4.0 N-m-s/rad
Axel damping coefficients	$b_{\rm F} = b_{\rm R}$	1000 N-m-s/rad
Axel stiffnesses	$k_{\rm F} = k_{\rm R}$	4000 N-m/rad
Wheel radii	$R_{\rm F} = R_{\rm R}$	0.45 m
EM gear ratio	$\tau_{\rm EM}$	0.3534
Differential ratios	$\tau_{\rm DF} = \tau_{\rm DR}$	0.2778
Transmission gear ratios	g $\tau_{\rm T}(g)$	1 2 3 4 5 3.38 2.04 1.3 1 0.78

TABLE I
Model Parameters

B. Simulation result plots

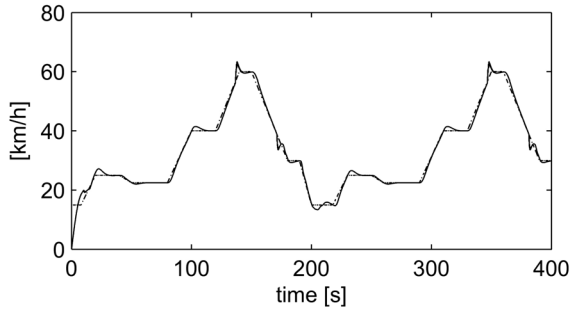

Fig. 3. Desired (dashed) versus actual (solid) vehicle speed, $x_4 = \dot{x}_{\rm v}$.

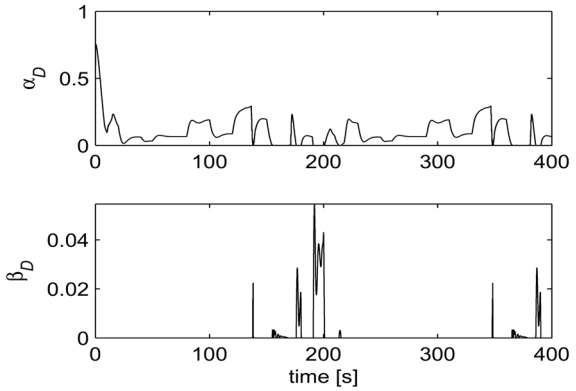

Fig. 4. Normalized driver accelerator pedal angle, α_D, and normalized brake pedal angle, β_D.

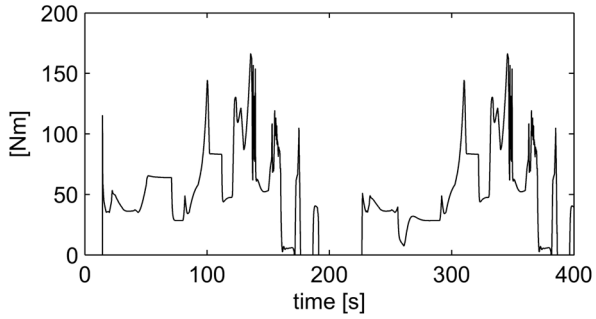

Fig. 5. Demanded ICE torque, $u_1 = T_{\mathrm{ICE}}$.

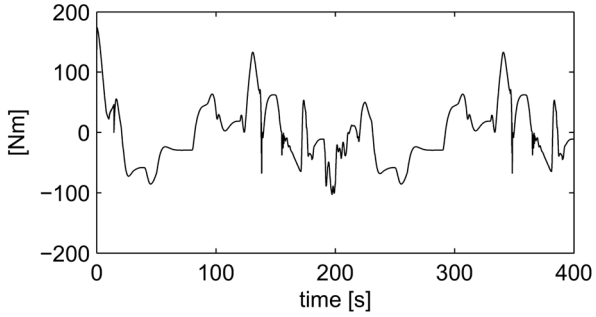

Fig. 6. Demanded EM torque, $u_3 = T_{\mathrm{EM}}$.

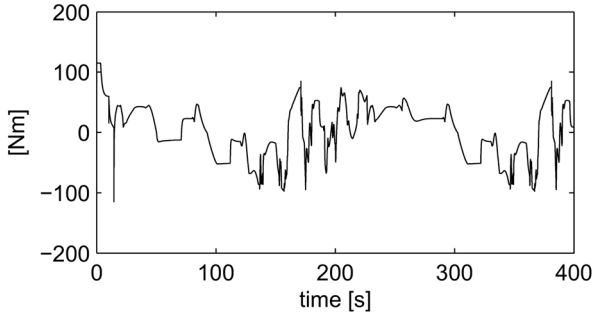

Fig. 7. Demanded ISA torque, $u_2 = T_{\mathrm{ISA}}$.

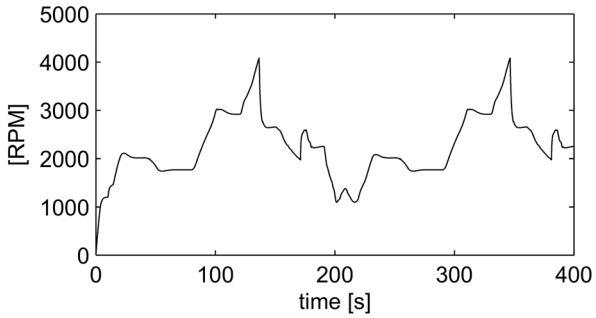

Fig. 8. ICE speed, $x_1 = \omega_{\mathrm{ICE}}$. Since the ICE and ISA are on a common shaft, the ICE speed equals the ISA speed.

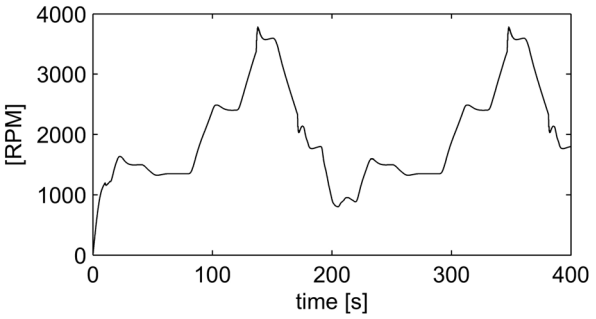

Fig. 9. EM speed, $x_3 = \omega_{\mathrm{EM}}$.

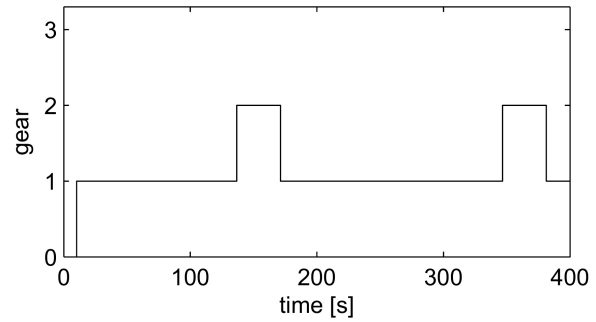

Fig. 10. Selected automatic transmission gear index, g.

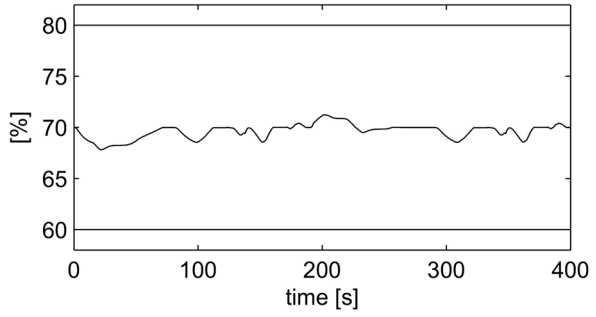

Fig. 11. Battery SOC, s. Note, $s_l = 0.6$ and $s_u = 0.8$.

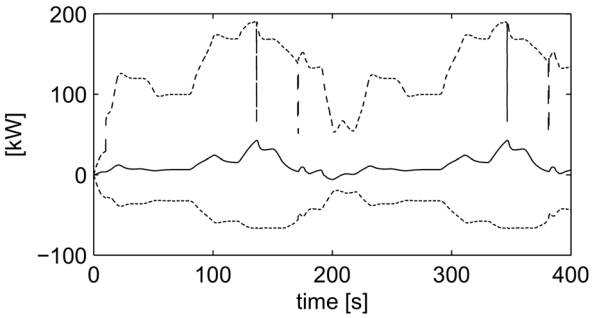

Fig. 12. Instantaneous power demand, P_{inst}, (solid), and the instantaneous maximum, $P^{\max}$, and minimum, $P^{\min}$, power available (dashed).